

# 1 Genomic characterization of a lumpy skin disease virus isolated in southeast China

2

3 Jun Ma<sup>1,3#</sup>, Yaoxian Yuan<sup>1,3#</sup>, Jianwei Shao<sup>1,3#</sup>, Minghui Sun<sup>1,3</sup>, Weinan Huang<sup>4,6</sup>, Xu Zhang<sup>1,3</sup>,  
4 Wei He<sup>5</sup>, Chunhua Huang<sup>4</sup>, Wencheng Xu<sup>4</sup>, Nanshan Qi<sup>2</sup>, Junwei Lin<sup>4</sup>, Jiming Chen<sup>1,3\*</sup>, Mingfei  
5 Sun<sup>2\*</sup>, Quan Liu<sup>1,3\*</sup>

6

7 1. School of Life Sciences and Engineering, Foshan University, Foshan, 528225, China

8 2. Key Laboratory of Livestock Disease Prevention of Guangdong Province, Maoming Branch,

9 Guangdong Laboratory for Lingnan Modern Agriculture, Scientific Observation and

10 Experiment Station of Veterinary Drugs and Diagnostic Techniques of Guangdong Province,

11 Ministry of Agriculture, Institute of Animal Health, Guangdong Academy of Agricultural

12 Sciences, Guangzhou 510640, China

13 3. Science and Technology Incubator, Foshan University, Foshan, 528225, China

14 4. Jieyang Animal Health Supervision Institute, Jieyang, 522000, China

15 5. Guangzhou Institute of Microbiology Co., Ltd, Guangzhou, 510000, China

16 6. Agricultural and Rural Bureau of Huilai County, Jieyang, 522000, China

17

18

19

## 20 SUMMARY

21 Lumpy skin disease virus (LSDV) is of high economic importance and has spread rapidly

22 to many European and Asian countries in recent years. LSDVs spread to China in 2019 and

23 have caused severe outbreaks in multiple provinces. The LSDVs in China have not been well

24 investigated. Here we isolated an LSDV (GD01/2020) in southeast China and investigated its

25 features in replication, phylogenetics, and genomics. GD01/2020 caused a typical LSD

26 outbreak and replicated well in MDBK cells as detected by a novel quantitative real-time PCR

27 assay targeting the viral GPCR gene. GD01/2020 was similar in phylogenetics to the one

28 circulating in Xinjiang, China in 2019, and distinct from the LSDVs identified in other countries.

29 In genomics, GD01/2020 was a vaccine-recombinant similar to those identified in Russia. A

30 total of 13 major putative recombination events between a vaccine strain and a field strain were

31 identified in the genome of GD01/2020, which could affect the virulence and transmissibility

32 of the virus. The results suggested that the LSD outbreaks in China caused by a virulent vaccine-

33 recombinant LSDV from the same unknown exotic source, and virulent vaccine-recombinant

34 LSDVs obtained transboundary transmissibility. This report shed novel insights into the

35 diagnosis, transmission, and control of the disease.

## 36 Introduction

37 Lumpy skin disease (LSD) has been listed as a notifiable viral disease of cattle by the  
38 World Organization for Animal Health (OIE). It is a serious transboundary disease and causes  
39 significant economic losses from decreased milk production, abortions, infertility, and damaged  
40 hides. Farmers in developing countries whose livelihood rely on cattle bear the heaviest burden  
41 (Babiuk et al., 2008). The etiological agent of LSD is lumpy skin disease virus (LSDV), a  
42 member of the genus *Capripoxvirus* within the family *Poxviridae*. It is genetically similar to  
43 the other two *Capripoxvirus* species Goatpox virus (GTPV) and Sheeppox virus (SPPV). LSDV  
44 harbors a double-stranded DNA genome, which is about 151,000 bp in size, encoding  
45 approximately 156 proteins (Tulman et al., 2001). LSDV is mainly transmitted via arthropod  
46 vectors, such as flies, mosquitos, and ticks (Chihota, Rennie, Kitching, & Mellor, 2001;  
47 Lubinga et al., 2015; Sprygin, Pestova, Wallace, Tuppurainen, & Kononov, 2019). Other  
48 transmission pathways, such as direct or indirect contact between infected and susceptible  
49 animals, were also possible (Aleksandr et al., 2020; Carn & Kitching; Sprygin et al., 2019).

50 LSD was first described in Zambia in 1929, and spread slowly in Africa thereafter  
51 (Davies, 1982). In 1989, LSD spread to Israel and subsequently circulated in the Middle East  
52 (Rweyemamu et al., 2000). In 2013, LSD spread to Europe and subsequently circulated in 11  
53 European countries, including Turkey, Greece, and Russia (Sevik & Dogan, 2017; Sprygin,  
54 Pestova, Prutnikov, & Kononov, 2018; Tasioudi et al., 2016). From 2019 on, outbreaks of  
55 LSD have been reported by several Asian countries, such as China, India, Bangladesh, and  
56 Nepal (Acharya & Subedi, 2020; Lu et al., 2020; Sudhakar et al., 2020).

57 Live attenuated vaccines (LAVs) were widely used for LSD control in various countries,  
58 such as Greece, Serbia, Croatia, Kazakhstan, and Armenia (Agianniotaki et al., 2017; Sprygin,  
59 Babin, et al., 2018; Tasioudi et al., 2016). These LAVs were developed by serially passing a  
60 Neethling-type field isolate in tissue culture and embryonated chicken eggs (Hunter &  
61 Wallace, 2001). Some LAV strains caused clinical symptoms in South Africa (van Schalkwyk  
62 et al., 2020). Moreover, two LAV recombinant stains, Saratov/Russia/2017 and  
63 Udmurtiya/Russia/2017, caused typical outbreaks of LSD in Russia (Sprygin, Babin, et al.,  
64 2018; Sprygin et al., 2020).

65 In July 2019, LSD outbreak was first identified in Xinjiang, northwest China, near to  
66 Kazakhstan and Russia. Despite great efforts to contain the disease, this disease spread to  
67 southeast China in 2020 and caused outbreaks in multiple provinces (Lu et al., 2020)  
68 (Appendix Figure 1). It remains unknown the genomic and other features of the LSDVs  
69 circulating in China. To address this issue, we isolated an LSDV in southeast China and  
70 investigated its features in replication, phylogenetics, and genomics.

71

## 72 **Materials and Methods**

### 73 **Sample collection**

74 A suspected LSD outbreak on a cattle herd with 70 animals was reported in June 2020 in  
75 southeast China. Skin nodules ( $n=23$ ), skin wound swabs ( $n=19$ ), Ocular swabs ( $n=17$ ), nasal  
76 swabs ( $n=16$ ), oral swabs ( $n=19$ ) and rectal swabs ( $n=14$ ) were collected from the affected cattle  
77 ( $n=6$ ). All the samples were immediately immersed in 1 mL of RPMI medium 1640 (Gibco,  
78 USA). These samples were crushed with a sterile grinder, and then suspended as 10%  
79 homogenates with RPMI medium 1640 and 1% antibiotic solution (penicillin G-sodium 100  
80 IU/mL and streptomycin sulphate 100 mg/mL), for DNA extraction and virus isolation.

### 81 **Viral DNA detection**

82 DNA were extracted by TIANamp Genomic DNA Kit (TIANGen, China) according to the  
83 manufacturer's instruction. The extracted DNA was detected by polymerase chain reaction  
84 (PCR) targeting the RPO30 and GPCR genes using the primers as described previously  
85 ((Lamien et al., 2011; Le Goff et al., 2009). The positive amplicons were sequenced for  
86 phylogenetic analysis. To quantitate LSDV genomic copies, a quantitative real-time PCR  
87 (qPCR) assay was developed using SYBR Green I targeting the viral GPCR gene. The qPCR  
88 was performed in a volume of 20  $\mu$ L containing 500 nM each primer, 1 $\times$ TB green Premix  
89 DimerEraser (Takara, China), and 2  $\mu$ L of DNA template. The amplification was conducted at  
90 95°C for 30 s, followed by 40 cycles of 95°C for 5 s, 60°C for 30 s, and 72°C for 30 s. The  
91 sample was considered positive if the cycle threshold was less than 31.3. The PCR primers used  
92 in this study are showed in Appendix Table 1.

### 93 **Virus isolation**

94 Madin-Darby bovine kidney (MDBK) cells were used for virus isolation as described  
95 previously (Fay et al., 2020). Briefly, MDBK cells were cultured in 1640 medium supplemented  
96 with 10% fetal bovine serum (Gibco, USA). The sample homogenates described above were  
97 inoculated onto the confluent cell monolayer for 2 hours, then the cells were washed with  
98 phosphate-buffered saline (PBS) for three times, followed by addition of fresh growth medium  
99 and incubated at 37°C in 5% CO<sub>2</sub>. Viral-induced cytopathic effects (CPE) were monitored for  
100 10 days following the inoculation. The supernatants were also collected for transmission  
101 electron microscopy as described previously (Wang et al., 2019).

### 102 **Virus replication kinetics**

103 To evaluate the replication kinetics of the virus, MDBK cells were cultured in 24-well  
104 plates using a multiplicity of infection (MOI) of 1.0 and 0.2, respectively. The virus was  
105 harvested at every 24 hours till the 7 days post infection (dpi), and its titer was quantified using

106 the qPCR.

## 107 **Genomic sequencing**

108 Whole-genome sequencing was performed on the Illumina HiSeq PE150 platform. To  
109 assemble the genome, reads were mapped to the reference genome (Saratov/Russia/2017,  
110 MH646674) and the assembled whole genomic sequence was stored in GenBank (accession  
111 number: MW355944).

## 112 **Phylogenetic analysis**

113 Sequence alignment was conducted by the MAFFT software tool (Katoh & Standley,  
114 2013). Phylogenetic relationships were calculated using the software package Mega X (Kumar,  
115 Stecher, Li, Knyaz, & Tamura, 2018), with the maximum likelihood method and the substitution  
116 model which was of the lowest Bayesian-Information-Criterion scores (the Tamura 3-parameter  
117 model for the GPCR gene sequences, the Hasegawa-Kishino-Yano model for the RPO30 gene  
118 sequences, and the General Time Reversible model for the genomic sequences). Rates among  
119 sites were set in gamma distribution. Bootstrap values were calculated with 1000 replicates.

## 120 **Recombination analysis**

121 For the recombination analysis, LSDV genomic sequences were aligned and analyzed  
122 using the bootscan/rescan recombination test (Martin, Posada, Crandall, & Williamson, 2005),  
123 MAXCHI (Smith, 1992), GENECONV (Padidam, Sawyer, & Fauquet, 1999), CHIMAERA  
124 (Posada & Crandall, 2001), and the SISCAN (Gibbs, Armstrong, & Gibbs, 2000) methods  
125 within the RDP software package (v4.39) with default settings. The SimPlot software was used  
126 to further characterize the potential recombinant events (Lole et al., 1999).

127

## 128 **Results**

### 129 **Field observation**

130 We observed that 24 of 70 (34.3%) cattle presented typical clinical signs of LSD, including  
131 pyrexia, salivation, nasal and ocular discharges, and skin nodules (1–2 cm to 7–8 cm in  
132 diameter). The skin nodules involved the epidermis, dermis, subcutis, and musculature with the  
133 appearance of ulcerations and deep scabs (Figure 1). No death was reported in this outbreak.

### 134 **Virus detection and isolation**

135 All clinical samples were tested by the PCR and qPCR assays, then further inoculated into  
136 MDBK cells for virus isolation. Of these samples, 7.1–91.3% were positive for the qPCR  
137 detection and 0.0–100.0% were positive for the virus isolation (Appendix Table 2, Figure 2).  
138 The LSDV was detected from all the types of collected samples, with high concentration in skin  
139 nodules, skin wound swabs, and ocular swabs (Appendix Figure 2). This suggests that LSDV  
140 could be transmitted through cattle-to-cattle direct contact or close contact with the virus shed

141 from skin wounds or body excretion or feces, which has been observed recently in Russia  
142 (Aleksandr et al., 2020).

143



144

145

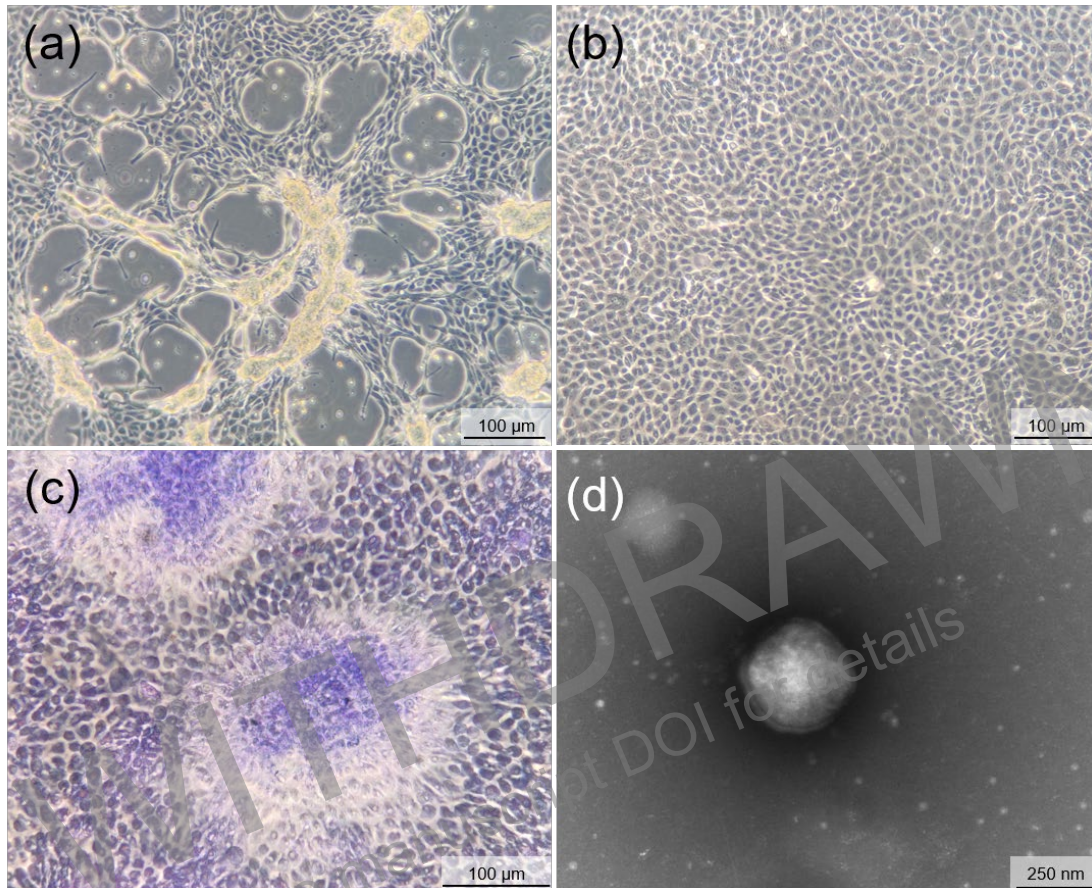
146 **Figure 1. Clinical signs of an LSD outbreak in southeast China.** (a, b) Skin nodules covering  
147 the entire body of infected cattle; (c, d) The necrotic wounds of skin subject to fly pestering.

148

149

150 LSDV was tough to be isolated until MDBK cells were found to be sensitive for the virus  
151 culture (Fay et al., 2020). In this study, we found that GD01/2020 replicated well in MDBK  
152 cells (Appendix Figure 3). This confirmed that MDBK cells could be used for the viral culture,  
153 disease diagnosis, and neutralizing antibodies quantification. Typical foci-type plaques were  
154 observed in infected MDBK cells after three times of blind passage. The foci-type plaques  
155 became visible at 2–4 dpi (Figure 2a, b), and were highlighted by crystal violet staining (Figure  
156 2c). LSDV virions in the supernatant were confirmed by the qPCR and transmission electron  
157 microscopy (Figure 2d). The LSDV isolate was designated as LSDV/GD01/China/2020  
158 (GD01/2020).

159



160

161 **Figure 2. Isolation of LSDV in MDBK cells.**

162 (a) The foci-type plaques in MDBK cells at 4 dpi with inoculated LSDV at a MOI of 1. (b)  
163 Uninfected MDBK cells. (c) The foci-type plaques in MDBK cells highlighted by crystal violet  
164 staining. (d) Negatively stained virions purified from LSDV-infected MDBK cells.

165

166

### 167 **Phylogenetic analysis**

168 We searched through the BLAST tool of NCBI, and found that GD01/2020 was the most  
169 similar to the LSDVs identified in Xinjiang, northwest China in 2019 in the RPO30 and GPCR  
170 gene sequences (similarity in the RPO30 gene sequences = 100.0%; similarity in the GPCR  
171 gene sequences = 99.9%). Phylogenetic analysis of these two genes showed that GD01/2020  
172 and the LSDVs from Xinjiang, northwest China formed a distinct clade between the vaccine-  
173 associated virus group and the field virus group (**Figure 3**), and surprisingly, they were distinct  
174 from the LSDVs identified in Kazakhstan, India, Bangladesh, and Russia. This result suggests  
175 that GD01/2020 and the LSDVs from Xinjiang/2019, northwest China likely had the same  
176 exotic source, and the source remains unknown.

177 **Figure 3** suggested that the nucleotides in the genomes of the LSDVs in the field group or  
178 the vaccine-associated group substituted slowly, and hence it should be likely for the LSDVs in

179 China to form a distinct clade through recombination rather than through nucleotide substitution.  
180 This is supported by **Appendix Table 3** which shows that the LSDVs in China shared the same  
181 nucleotides with the field virus group in a region of each of the genes and shared the same  
182 nucleotides with the vaccine-associated group in other regions of the genes, far from a random  
183 distribution, which constituted a marked signal of recombination. **Figure 3** also showed that,  
184 as per the sequences of GPCR and RPO30, the LSDVs in China were distinct from the two  
185 vaccine-recombinant stains, Saratov/Russia/2017 and Udmurtiya/Russia/2017, causing typical  
186 outbreaks of LSD in Russia (Sprygin, Babin, et al., 2018; Sprygin et al., 2020).

187

### 188 **Genomic analysis**

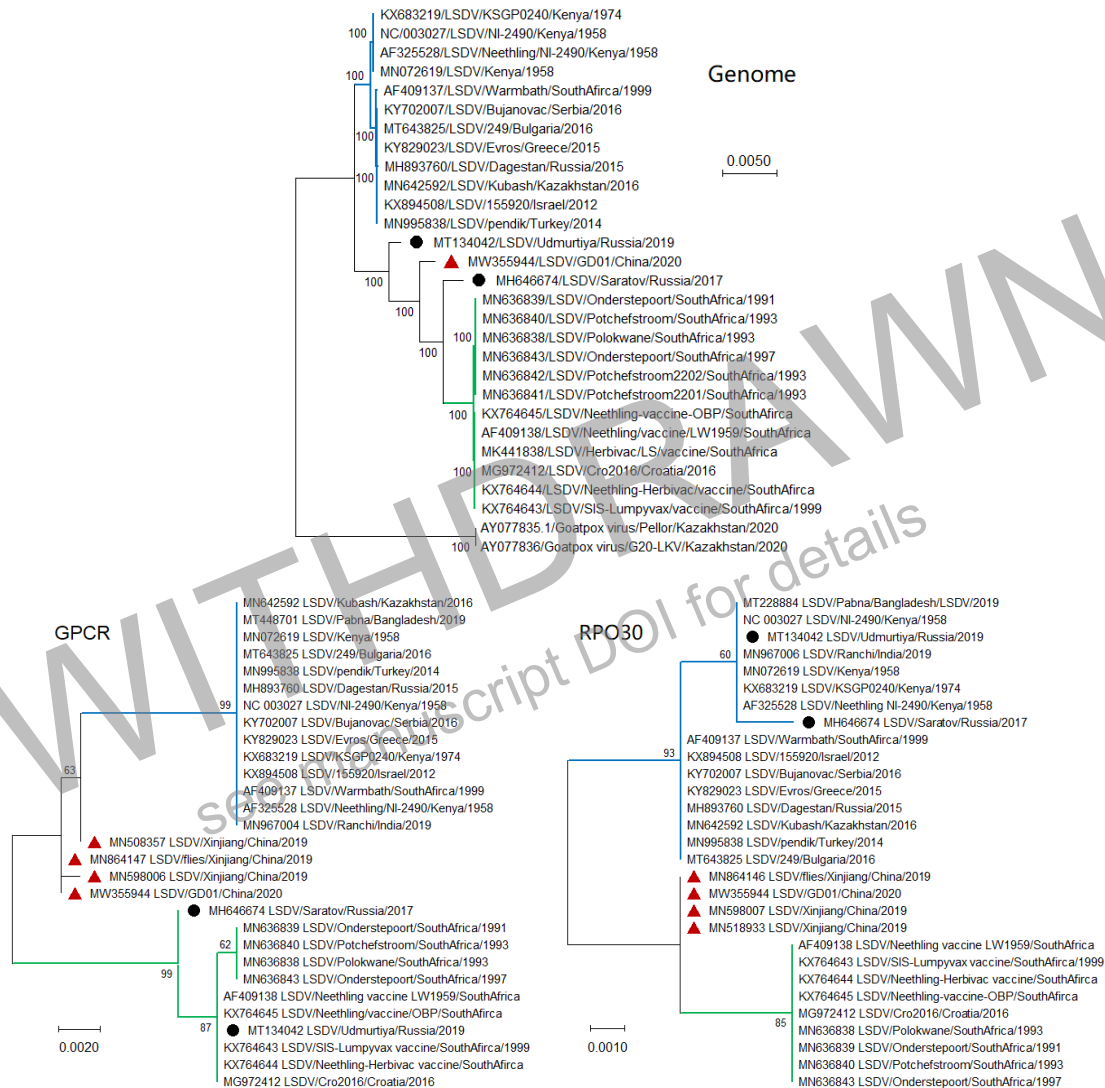
189 The genome of GD01/2020 was sequenced using the metagenomic method, which  
190 produced 2,957,618 reads assembled into a 150606-nt contig. Phylogenetic analysis based on  
191 all available complete genomic sequences of LSDVs showed that GD01/2020 clustered  
192 between the vaccine-associated virus group and the field virus group, and between the two  
193 recombinant viruses, Saratov/Russia/2017 and Udmurtiya/Russia/2017, reported in Russia  
194 (**Figure 3**). Pairwise comparisons showed that GD01/2020 had a higher similarity with these  
195 two Russian LSDV recombinant viruses (99.4%) than other viruses (99.2–99.3%). These  
196 results indicated that GD01/2020 was likely a recombinant LSDV strain.

197

198

199

200



201

202

203 **Figure 3.** Phylogenetic relationships among some LSDVs based on their whole genomic  
 204 sequences, GPCR gene sequences, or RPO30 gene sequences. The LSDVs from China are  
 205 marked with triangles; the field group is marked with blue branches; the vaccine-associated  
 206 group is marked with green branches. Two Russia isolates are marked with black circles. Scale  
 207 bars indicate genetic distances.

208

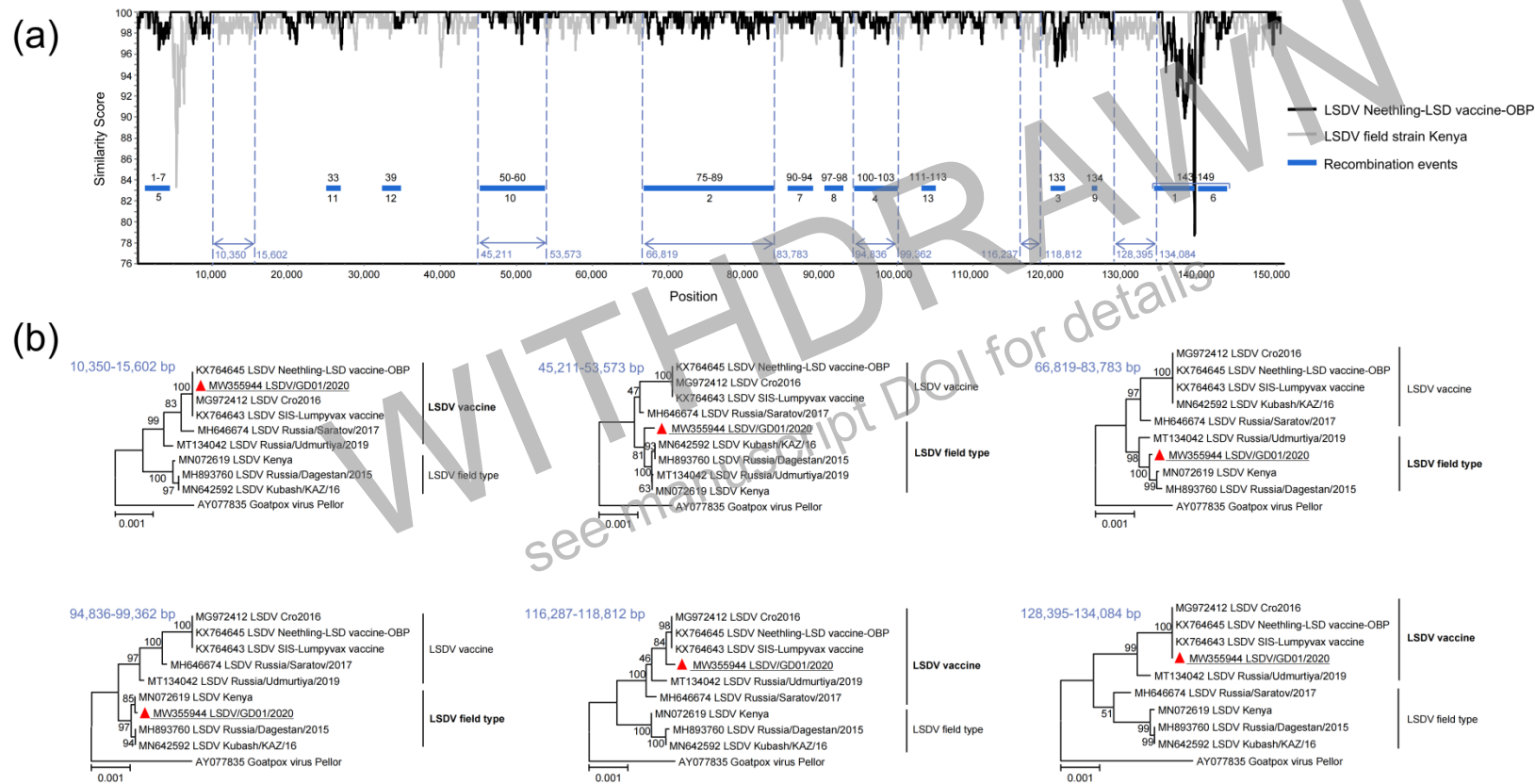
### 209 Recombination analysis

210 Genomic sequences of 18 LSDVs were analyzed using the RDP program. The results  
 211 further supported that GD01/2020 was a recombinant virus, with vaccine strains as the  
 212 putative major parent donors and field strains as the putative minor parent donors (**Appendix**  
 213 **Table 4**).



214 The similarity plot of the full-length genome of GD01/2020 was further analyzed using  
215 the LSDV reference sequences of the Neethling vaccine strain OBP (MG972412) and the  
216 LSDV field strain Kenya (MN072619). A total of 13 major putative recombination events  
217 involving dozens of proteins were found (**Figure 4, Appendix Table 5**). All of the putative  
218 recombination events had a vaccine virus genome as the major parental donor and a field  
219 virus as the minor parental donor. Moreover, the termination codons of five genes of  
220 GD01/2020, ORF086, ORF087, ORF131, ORF134, and ORF144, changed as compared with  
221 the Neethling vaccine strain OBP. The open reading frames (ORFs) of these genes were  
222 extended thereby (Appendix Figure 4).

WITHDRAWN  
see manuscript DOI for details



223  
 224 **Figure 4. Recombination analysis of the genomes of LSDVs.** (a) Similarity plot of the genomic sequence of GD01/2020 compared to the  
 225 Neethling vaccine strain OBP (in black) and the LSDV field strain Kenya (in gray); the blue boxes show the positions of the predicted recombination  
 226 events; the numbers on the boxes show the order of the viral proteins affected by the recombination events (e.g., 1–7 means the viral proteins  
 227 ORF001–ORF007); the numbers below the boxes show the order of the recombination events. The sequences chosen for phylogenetic analysis are  
 228 indicated by blue arrows; (b) Phylogenetic relationships based on the sequences of the selected six regions; sequence positions are marked in blue  
 229 and GD01/2020 is marked with a triangle.

## 230 **Discussion**

231 Our field observation in this study suggested that the affected cattle were of typical clinical  
232 signs of LSD, and thus the isolated LSDV (GD01/2020) was virulent. Phylogenetic analysis of  
233 two genes (GPCR and RPO30) suggested that GD01/2020 and the LSDV caused the LSD  
234 outbreaks in Xinjiang, China in 2019 were vaccine-recombinants and likely from the same  
235 unknown exotic source. Genomic sequence analysis suggested that GD01/2020 was a vaccine-  
236 recombinant similar to the two vaccine-recombinants identified in Russia in 2017 and 2019  
237 (Sprygin, Babin, et al., 2018; Sprygin et al., 2020).

238 Live attenuated LSD vaccines have been in use in Africa for decades. They have also been  
239 used in multiple affected countries in the northern hemisphere, including Serbia, Croatia,  
240 Kazakhstan, and Armenia (Sprygin, Babin, et al., 2018). Because only heterologous live  
241 goatpox or sheeppox vaccines have been permitted for the control of LSD in Russia and China,  
242 and live LSD vaccines have not been permitted for use in Russia and China, these vaccine-  
243 recombinant LSDVs likely emerged in other countries where live LSD vaccines have been used.  
244 Therefore, virulent vaccine-recombinant LSDVs likely caused transboundary transmission to  
245 these two countries and had transboundary transmissibility thereby.

246 It has been found that vaccine-recombinant LSDVs increased the viral virulence as  
247 compared with a field LSDV (Kononova et al., 2020), and could be transmitted through direct  
248 or indirect contact (Aleksandr et al., 2020). These findings provided the explanation for the  
249 potential transboundary transmissibility of vaccine-recombinant LSDVs. They also indicated  
250 that more caution should be given in using live LSDV vaccines for control of the disease. This  
251 study suggested that virulent vaccine-recombinant LSDVs likely spread from northwest China  
252 to southeast China within one year, further supporting that virulent vaccine-recombinant  
253 LSDVs can spread rapidly.

254 Consistent with previous studies (Sprygin, Babin, et al., 2018; Sprygin et al., 2020), the  
255 genomic recombination of GD01/2020 involved dozens of proteins of the virus (Appendix  
256 Table 4). It is valuable to investigate in the future which proteins are important for the virulence  
257 and transmissibility of the virus.

258 In summary, we isolated a virulent vaccine-recombinant LSDV in southeast China, and

259 investigated the viral features in replication, phylogenetics, and genomics. The results shed  
260 novel insights into the diagnosis, transmission, and control of the disease, and suggested that  
261 vaccine-recombinant LSDVs likely caused transboundary transmission to Russia and China.  
262 More national and international efforts to investigate and contain virulent vaccine-recombinant  
263 LSDVs are desirable.

264

## 265 **Acknowledgements**

266 This study was supported by the Pearl River Talent Plan in Guangdong Province of China  
267 (2019CX01N111).

## 268 **Conflict of Interest Statement**

269 The authors have declared no conflict of interest.

270

## 271 **References**

- 272 Acharya, K. P., & Subedi, D. (2020). First outbreak of lumpy skin disease in Nepal. *Transbound Emerg Dis*,  
273 67(6), 2280-2281. doi:10.1111/tbed.13815
- 274 Agianniotaki, E. I., Tasioudi, K. E., Chaintoutis, S. C., Iliadou, P., Mangana-Vougiouka, O., Kirtzalidou, A., . . .  
275 Chondrokouki, E. (2017). Lumpy skin disease outbreaks in Greece during 2015-16, implementation of  
276 emergency immunization and genetic differentiation between field isolates and vaccine virus strains. *Vet*  
277 *Microbiol*, 201, 78-84. doi:10.1016/j.vetmic.2016.12.037
- 278 Babiuk, S., Bowden, T. R., Parkyn, G., Dalman, B., Manning, L., Neufeld, J., . . . Boyle, D. B. (2008).  
279 Quantification of lumpy skin disease virus following experimental infection in cattle. *Transbound Emerg*  
280 *Dis*, 55(7), 299-307. doi:10.1111/j.1865-1682.2008.01024.x
- 281 Carn, V. M., & Kitching, R. P. (1995). An investigation of possible routes of transmission of lumpy skin disease  
282 virus (Neethling). *Epidemiol Infect*, 114(1), 219-226. doi:10.1017/s0950268800052067
- 283 Chihota, C. M., Rennie, L. F., Kitching, R. P., & Mellor, P. S. (2001). Mechanical transmission of lumpy skin  
284 disease virus by *Aedes aegypti* (Diptera: Culicidae). *Epidemiol Infect*, 126(2), 317-321.  
285 doi:10.1017/s0950268801005179
- 286 Davies, F. G. (1982). Observations on the epidemiology of lumpy skin disease in Kenya. *J Hyg (Lond)*, 88(1),  
287 95-102. doi:10.1017/s002217240006993x
- 288 Fay, P. C., Cook, C. G., Wijesiriwardana, N., Tore, G., Comtet, L., Carpentier, A., . . . Beard, P. M. (2020).  
289 Madin-Darby bovine kidney (MDBK) cells are a suitable cell line for the propagation and study of the  
290 bovine poxvirus lumpy skin disease virus. *J Virol Methods*, 285, 113943.  
291 doi:10.1016/j.jviromet.2020.113943
- 292 Gibbs, M. J., Armstrong, J. S., & Gibbs, A. J. (2000). Sister-scanning: a Monte Carlo procedure for assessing  
293 signals in recombinant sequences. *Bioinformatics*, 16(7), 573-582. doi:10.1093/bioinformatics/16.7.573
- 294 Hunter, P., & Wallace, D. (2001). Lumpy skin disease in southern Africa: a review of the disease and aspects of  
295 control. *J S Afr Vet Assoc*, 72(2), 68-71. doi:10.4102/jsava.v72i2.619
- 296 Katoh, K., & Standley, D. M. (2013). MAFFT multiple sequence alignment software version 7: improvements in

- 297 performance and usability. *Mol Biol Evol*, 30(4), 772-780. doi:10.1093/molbev/mst010
- 298 Kimura, M. (1980). A simple method for estimating evolutionary rates of base substitutions through comparative  
299 studies of nucleotide sequences. *J Mol Evol*, 16(2), 111-120. doi:10.1007/BF01731581
- 300 Kumar, S., Stecher, G., Li, M., Knyaz, C., & Tamura, K. (2018). MEGA X: Molecular Evolutionary Genetics  
301 Analysis across Computing Platforms. *Mol Biol Evol*, 35(6), 1547-1549. doi:10.1093/molbev/msy096
- 302 Lole, K. S., Bollinger, R. C., Paranjape, R. S., Gadhari, D., Kulkarni, S. S., Novak, N. G., . . . Ray, S. C. (1999).  
303 Full-length human immunodeficiency virus type 1 genomes from subtype C-infected seroconverters in  
304 India, with evidence of intersubtype recombination. *J Virol*, 73(1), 152-160. doi:10.1128/JVI.73.1.152-  
305 160.1999
- 306 Lu, G., Xie, J., Luo, J., Shao, R., Jia, K., & Li, S. (2020). Lumpy skin disease outbreaks in China, since 3 August  
307 2019. *Transbound Emerg Dis*. doi:10.1111/tbed.13898
- 308 Lubinga, J. C., Tuppurainen, E. S., Mahlare, R., Coetzer, J. A., Stoltz, W. H., & Venter, E. H. (2015). Evidence  
309 of transstadial and mechanical transmission of lumpy skin disease virus by *Amblyomma hebraeum* ticks.  
310 *Transbound Emerg Dis*, 62(2), 174-182. doi:10.1111/tbed.12102
- 311 Martin, D. P., Posada, D., Crandall, K. A., & Williamson, C. (2005). A modified bootscan algorithm for  
312 automated identification of recombinant sequences and recombination breakpoints. *AIDS Res Hum*  
313 *Retroviruses*, 21(1), 98-102. doi:10.1089/aid.2005.21.98
- 314 OIE. (2018). Lumpy skin disease. chapter 3.04.12. In P. Beard & B.A. Lubisi (Eds.), *OIE terrestrial manual* (pp.  
315 1158–1171). Paris, France: World Organization for Animal Health.
- 316 Padidam, M., Sawyer, S., & Fauquet, C. M. (1999). Possible emergence of new geminiviruses by frequent  
317 recombination. *Virology*, 265(2), 218-225. doi:10.1006/viro.1999.0056
- 318 Posada, D., & Crandall, K. A. (2001). Evaluation of methods for detecting recombination from DNA sequences:  
319 computer simulations. *Proc Natl Acad Sci U S A*, 98(24), 13757-13762. doi:10.1073/pnas.241370698
- 320 Rweyemamu, M., Paskin, R., Benkirane, A., Martin, V., Roeder, P., & Wojciechowski, K. (2000). Emerging  
321 diseases of Africa and the Middle East. *Ann N Y Acad Sci*, 916, 61-70. doi:10.1111/j.1749-  
322 6632.2000.tb05275.x
- 323 Saitou, N., & Nei, M. (1987). The neighbor-joining method: a new method for reconstructing phylogenetic trees.  
324 *Mol Biol Evol*, 4(4), 406-425. doi:10.1093/oxfordjournals.molbev.a040454
- 325 Sevik, M., & Dogan, M. (2017). Epidemiological and Molecular Studies on Lumpy Skin Disease Outbreaks in  
326 Turkey during 2014-2015. *Transbound Emerg Dis*, 64(4), 1268-1279. doi:10.1111/tbed.12501
- 327 Smith, J. M. (1992). Analyzing the mosaic structure of genes. *J Mol Evol*, 34(2), 126-129.  
328 doi:10.1007/BF00182389
- 329 Sprygin, A., Babin, Y., Pestova, Y., Kononova, S., Wallace, D. B., Van Schalkwyk, A., . . . Kononov, A. (2018).  
330 Analysis and insights into recombination signals in lumpy skin disease virus recovered in the field. *PLoS*  
331 *One*, 13(12), e0207480. doi:10.1371/journal.pone.0207480
- 332 Sprygin, A., Pestova, Y., Prutnikov, P., & Kononov, A. (2018). Detection of vaccine-like lumpy skin disease  
333 virus in cattle and *Musca domestica* L. flies in an outbreak of lumpy skin disease in Russia in 2017.  
334 *Transbound Emerg Dis*, 65(5), 1137-1144. doi:10.1111/tbed.12897
- 335 Sprygin, A., Pestova, Y., Wallace, D. B., Tuppurainen, E., & Kononov, A. V. (2019). Transmission of lumpy  
336 skin disease virus: A short review. *Virus Res*, 269, 197637. doi:10.1016/j.virusres.2019.05.015
- 337 Sprygin, A., Van Schalkwyk, A., Shumilova, I., Nesterov, A., Kononova, S., Prutnikov, P., . . . Kononov, A.  
338 (2020). Full-length genome characterization of a novel recombinant vaccine-like lumpy skin disease virus  
339 strain detected during the climatic winter in Russia, 2019. *Arch Virol*, 165(11), 2675-2677.  
340 doi:10.1007/s00705-020-04756-7

- 341 Sudhakar, S. B., Mishra, N., Kalaiyarasu, S., Jhade, S. K., Hemadri, D., Sood, R., . . . Singh, V. P. (2020).  
342 Lumpy skin disease (LSD) outbreaks in cattle in Odisha state, India in August 2019: Epidemiological  
343 features and molecular studies. *Transbound Emerg Dis*, 67(6), 2408-2422. doi:10.1111/tbed.13579  
344 Tasioudi, K. E., Antoniou, S. E., Iliadou, P., Sachpatzidis, A., Plevraki, E., Agianniotaki, E. I., . . . Dile, C.  
345 (2016). Emergence of Lumpy Skin Disease in Greece, 2015. *Transbound Emerg Dis*, 63(3), 260-265.  
346 doi:10.1111/tbed.12497  
347 Tulman, E. R., Afonso, C. L., Lu, Z., Zsak, L., Kutish, G. F., & Rock, D. L. (2001). Genome of lumpy skin  
348 disease virus. *J Virol*, 75(15), 7122-7130. doi:10.1128/JVI.75.15.7122-7130.2001  
349 van Schalkwyk, A., Kara, P., Ebersohn, K., Mather, A., Annandale, C. H., Venter, E. H., & Wallace, D. B.  
350 (2020). Potential link of single nucleotide polymorphisms to virulence of vaccine-associated field strains of  
351 lumpy skin disease virus in South Africa. *Transbound Emerg Dis*, 67(6), 2946-2960.  
352 doi:10.1111/tbed.13670  
353 Wang, Z. D., Wang, B., Wei, F., Han, S. Z., Zhang, L., Yang, Z. T., . . . Liu, Q. (2019). A New Segmented Virus  
354 Associated with Human Febrile Illness in China. *N Engl J Med*, 380(22), 2116-2125.  
355 doi:10.1056/NEJMoa1805068  
356 Zhugunissov, K., Bulatov, Y., Orynbayev, M., Kutumbetov, L., Abduraimov, Y., Shayakhmetov, Y., . . .  
357 Tuppurainen, E. (2020). Goatpox virus (G20-LKV) vaccine strain elicits a protective response in cattle  
358 against lumpy skin disease at challenge with lumpy skin disease virulent field strain in a comparative study.  
359 *Vet Microbiol*, 245, 108695. doi:10.1016/j.vetmic.2020.108695  
360 Zhang, M. M., Sun, Y.J., Liu, R.Q., Wang, X.J., & Bu, Z., G. (2020). Isolation and identification of lumpy skin  
361 disease virus from the first outbreak in China. *Chinese Journal of Preventive Veterinary Medicine*, 42(10),  
362 1-4. [In Chinese]  
363

## Appendix

**Appendix Table 1.** The primers used for detection of LSDV in this study.

Target gene	Primer name	Position <sup>a</sup>	Sequence (5'-3')
GPCR	GPCR-F	7070–7099	TTTTTTTATTTTTTATCCAATGCTAATACT
	GPCR-R	8225–8253	TTAAGTAAAGCATAACTCCAACAAAAATG
RPO30	RPO30-F	27699–27720	ATTCGTTTATCGCAGAACAAGG
	RPO30-R	28910–28935	CACCAACCATAGAATAGTATTGAGAC
GPCR <sup>b</sup>	qGPCR-F	7928–7950	AGTCGAATATAAAGTAATCAGTC
	qGPCR-R	8028–8052	CCGCATATAATACTTATTATAG

<sup>a</sup> Numbered according to the reference strain Saratov/Russia/2017 (MH646674).

<sup>b</sup> The pair of primers used in the qPCR.

**Appendix Table 2.** Detection of LSDV in different clinical samples.

Type of samples	Sample number	qPCR positive rate (%)	Isolation positive rate (%)
Nodules	23	91.3	100.0
Skin wound swabs	19	73.7	94.7
Oral swabs	19	36.8	0.0
Nasal swabs	16	18.8	31.3
Ocular swabs	17	29.4	0.0
Rectal swabs	14	7.1	0.0
Total	108	47.2	42.6

**Appendix Table 3.** Nucleotide mutations in two genes of the LSDVs in China compared the field virus group and the vaccine-associated group<sup>a</sup>.

Gene	Position	LSDVs in China	Field virus group	Vaccine-associated group
GPCR	18	C	T	C
	87	C	T	C
	153	A	A	G
	159	G	G	A
	227	G	G	A
	228	C	C	T
	381	G	G	A
	394	T	T	C
	400	C	C	T
	492	T	T	C
	528	C	C	T
	555	T	T	C
	648	C	C	T
	803	C	C	T
	822	T	T	C
	849	C	A	C
	852	G	A	G
	983	C	T	C
	987	A	G	A
	991	A	C	C
1050	T	C	T	
1116	T	C	T	
RPO30	103	A	A	G
	210	C	C	T
	243	T	C	T
	420	C	T	C
	477	T	C	C
	582	A	G	A

<sup>a</sup> Those lines in blue show the positions where LSDVs in China shared the same nucleotides with the field virus group, and those lines in green show the positions where LSDVs in China shared the same nucleotides with the vaccine-associated group.



**Appendix Table 4.** Recombination events in the genome of GD01/2020 predicted as compared the genomic sequences of other 18 LSDVs.

Event	Positions	Size (bp)	The most likely minor parent contributing less nucleotides	The most likely major parent contributing more nucleotides	Affected proteins	P-value calculated using different methods in the RDP software package					
						RDP	GENECONV	Bootscan	Maxchi	Chimaera	SISscan
1	134908–139307	4399	MN072619/Kenya/1958	MN636839/Onderstepoort/SouthAfrica/1991	ORF143–ORF145	6.24E-47	3.79E-52	1.48E-52	5.83E-27	3.33E-26	4.20E-39
2	66880–83858	16978	MN072619/Kenya/1958	KX764645/Neethling-vaccine-OBP/SouthAfrica	ORF075–ORF089	7.54E-33	7.29E-33	4.98E-17	5.30E-13	5.27E-13	3.90E-11
3	120459–122549	2090	MN072619/Kenya/1958	KX764645/Neethling-vaccine-OBP/SouthAfrica	ORF133	1.22E-11	1.17E-08	1.35E-11	4.88E-09	4.85E-09	4.85E-04
4	94912–99362	4450	MN072619/Kenya/1958	KX764645/Neethling-vaccine-OBP/SouthAfrica	ORF100–ORF103	9.88E-13	4.12E-12	2.33E-12	1.06E-06	1.05E-06	NS
5	343–4411	4069	MN072619/Kenya/1958	KX764645/Neethling-vaccine-OBP/SouthAfrica	ORF001–ORF007	NS	2.85E-20	2.00E-14	9.50E-07	1.72E-06	NS
6	139929–144054	4125	MN072619/Kenya/1958	MN636839/Onderstepoort/SouthAfrica/1991	ORF146–ORF149	4.84E-13	1.18E-08	2.11E-05	1.64E-11	1.62E-11	NS
7	85731–89270	3539	KX683219/KSGP0240/Kenya/1974	AF409138/Neethling/vaccine/ORF1959/SouthAfrica	ORF090–ORF094	8.68E-07	1.59E-05	6.76E-05	1.29E-05	8.53E-06	NS
8	91420–92899	1479	MN072619/Kenya/1958	KX764645/Neethling-vaccine-OBP/SouthAfrica	ORF097–ORF098	NS <sup>a</sup>	9.68E-07	3.34E-08	3.38E-05	3.38E-05	NS
9	127999–128410	411	MH893760/Dagestan/Russia/2015	KX764644/Neethling-Herbivac/vaccine/SouthAfrica	ORF134	NS	1.30E-06	3.75E-03	NS	NS	2.92E-27
10	45262–53624	8362	KY702007/Bujanovac/Serbia/2016	AF409138/Neethling/vaccine/ORF1959/SouthAfrica	ORF050–ORF060	NS	1.78E-03	NS	1.95E-06	1.93E-06	4.54E-12
11	26759–27542	783	MN642592/Kubash/Kazakhstan/2016	KX764645/Neethling-vaccine-OBP/SouthAfrica	ORF033	NS	0.0004025	2.81E-04	NS	NS	NS
12	34010–35138	1128	MN072619/Kenya/1958	KX764645/Neethling-vaccine-OBP/SouthAfrica	ORF039	NS	1.37E-04	1.65E-05	NS	NS	NS
13	103506–104806	1300	MN072619/Kenya/1958	MK441838/Herbivac/LS/vaccine/SouthAfrica	ORF111–ORF113	NS	1.42E-04	1.56E-04	NS	NS	NS

<sup>a</sup> These 18 strains included 6 strains predicted as the major parents donating more nucleotides to GD01/2020 (they were all in the vaccine-associated group):

KX764643/LSDV/SIS-Lumpyvax/vaccine/SouthAfrica/1999, MG972412/LSDV/Cro2016/Croatia/2016, KX764644/LSDV/Neethling-Herbivac/vaccine/SouthAfrica, AF409138/LSDV/Neethling/vaccine/ORF1959/SouthAfrica, KX764645/LSDV/Neethling-vaccine-OBP/SouthAfrica, MK441838/LSDV/Herbivac/LS/vaccine/SouthAfrica.

These 18 strains also include 12 strains predicted as the minor parents donating less nucleotides to GD01/2020 (they were all in the field virus group):

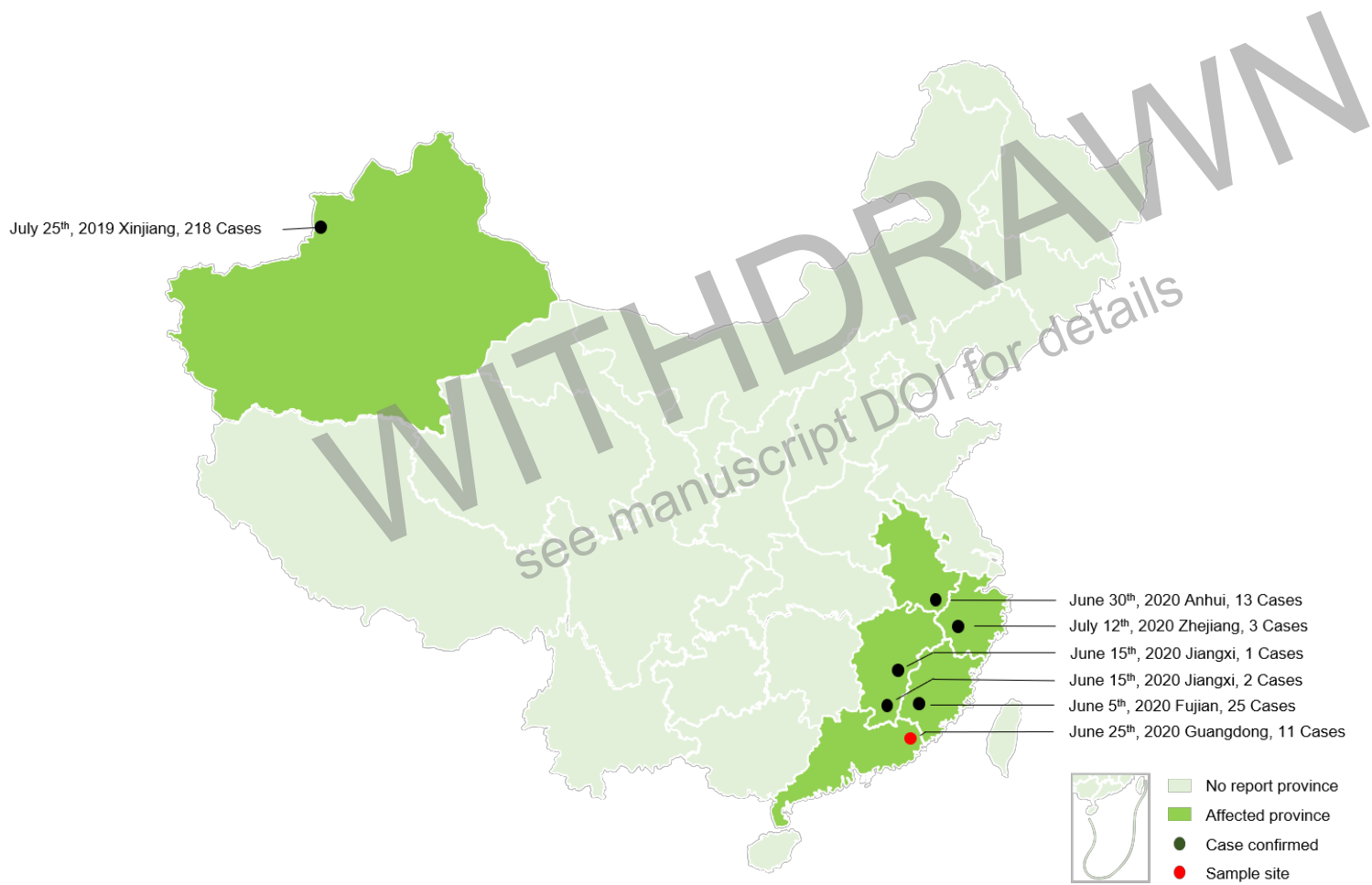
MN072619/LSDV/Kenya/1958, KX683219/LSDV/KSGP0240/Kenya/1974, NC/003027/LSDV/NI-2490/Kenya/1958, AF325528/LSDV/Neethling/NI-2490/Kenya/1958, AF409137/LSDV/Warmbath/SouthAfrica/1999, KY702007/LSDV/Bujanovac/Serbia/2016, MH893760/LSDV/Dagestan/Russia/2015, MT643825/LSDV/249/Bulgaria/2016, KY829023/LSDV/Evros/Greece/2015, MN642592/LSDV/Kubash/Kazakhstan/2016, MN995838/LSDV/pendik/Turkey/2014, KX894508/LSDV/155920/Israel/2012.

<sup>b</sup> NS, not statistically significant.

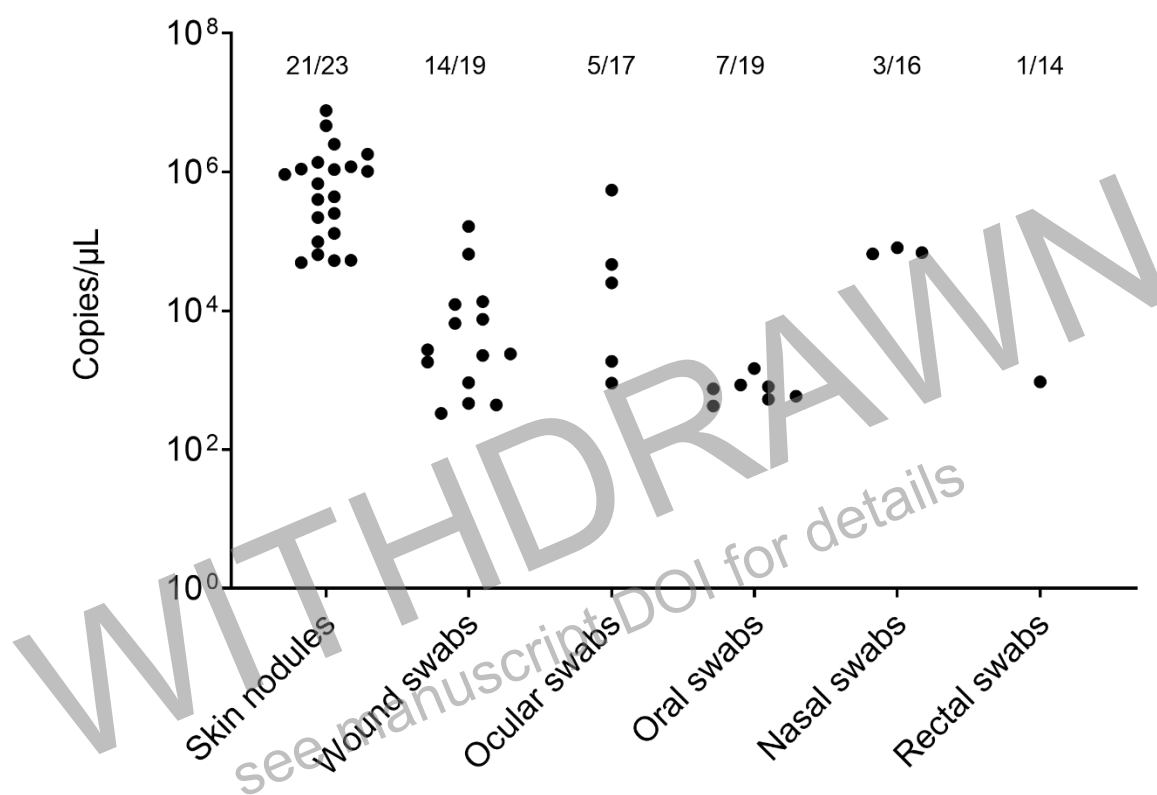
**Appendix Table 5.** The proteins of GD01/2020 affected by 13 major predicted genomic recombination events<sup>a</sup>.

Event	Amino acid differences between the predicted major parent KX764645/Neethling-vaccine-OBP/SouthAfrica and the predicted minor parent of MN072619/Kenya/1958
1	ORF143 (hypothetical protein): T267S; ORF144 (kelch-like protein): K51R, G78R, F119L, R139K, E195A, <u>I218D</u> , <u>S234N</u> , F252L, D257L, extension of the protein with 281 amino acid residues due to a change in the termination codon, <u>338Edel</u> , <u>Y374H</u> , <u>P384S</u> , <u>S422T</u> , <u>E455A</u> , <u>S518A</u> , <u>C538S</u> , F548L ORF145 (ankyrin repeat protein): I8V, <u>K22L</u> , <u>S121G</u> , <u>I139V</u> , <u>V144I</u> , <u>T181I</u> , <u>G196N</u> , <u>S202R</u> , <u>N205D</u> , <u>T210S</u> , <u>C216S</u> , <u>K241Q</u> , <u>M261V</u> , <u>V264I</u> , <u>L269I</u> , <u>N273S</u> , <u>S292N</u> , <u>S309N</u> , <u>V336I</u> , <u>I340V</u> , <u>H342N</u> , <u>D349E</u> , <u>Y353H</u> , <u>K378R</u> , <u>S385F</u> , <u>V416A</u> , <u>I457V</u> , <u>S461N</u> , <u>L472I</u> , <u>N481D</u> , <u>D502E</u> , <u>F511S</u> , <u>S512L</u> , <u>S516G</u> , <u>K561R</u> , <u>K564R</u> , <u>V575I</u> , <u>H599N</u> , <u>D611N</u> , <u>N615S</u> , <u>V624I</u>
2	ORF075 (RNA polymerase-associated protein): V324A; ORF076 (late transcription factor VLTF-4): V64A, 98DNdel, 103Ndel, <u>D151G</u> ; ORF079 (mRNA capping enzyme large subunit): I206T, D295N, T374P; ORF080 (hypothetical protein): I26M, T93I; ORF081 (putative virion protein): H17N, S227N; ORF082 (uracil DNA glycosylase): R54Q; ORF083 (putative NTPase): S3G, S49T, G106D, I135M, I253L, I708T; ORF084 (putative early transcription factor small subunit): L353V, D581N; ORF085 (RNA polymerase subunit): M136T; ORF086 (mutT motif): E121D, L191F, extension of the protein with 3 amino acid residues due to a change in the termination codon; Translation similar to minor parent, thus 207–213 NTLVNSK; ORF087 (mutT motif putative gene expression regulator): V46I, extension of the protein with 53 amino acid residues due to a change in the termination codon; ORF088 (putative transcription termination factor): I24V; ORF089 (mRNA capping enzyme small subunit): V171I
3	ORF133: V165I, <u>D200E</u> , S275N, L312S, <u>I344T</u> , <u>D347N</u> , <u>S514A</u> ; ORF134: <u>G2R</u>
4	ORF101: <u>E223D</u> ; ORF102: <u>A61N</u> , <u>L115S</u> , T162A; ORF103: <u>T50N</u> , P72T, S89G
5	ORF001: <u>V42E</u> , <u>D129V</u> , <u>I144M</u> ; ORF003: <u>S93T</u> , <u>A100S</u> ; ORF005: <u>15Fdel</u> , <u>A23V</u> , <u>I24V</u> ; ORF006: <u>F13L</u> , <u>S61L</u> , <u>95Sdel</u> , <u>I111S</u> , <u>S216N</u> ; ORF007: <u>S200T</u>
6	ORF146: <u>T285S</u> ; ORF147: <u>I487M</u> ; ORF148: <u>G40S</u> , <u>G51D</u> , <u>I102L</u> , <u>N167D</u> , <u>E169D</u> , <u>V351M</u> , <u>K361Q</u> , <u>C397Y</u> , <u>K413E</u> , <u>A418T</u> , <u>N439S</u> .
7	ORF093: <u>D60N</u> ; ORF094: <u>D93N</u> , <u>F607L</u>
8	ORF098: <u>I355V</u> , <u>R404H</u> , <u>I505V</u> , D553G, T652I
9	ORF134: L1973I, <u>2007Ndel</u> , extension of the protein with 59 amino acid residues due to a change in the termination codon
10	ORF050: 376Ndel; ORF054: <u>6 LP</u> ; ORF055: <u>M184I</u> ; ORF056: <u>K171R</u> ; <u>N174D</u> ; ORF057: <u>V372I</u> ; ORF059: Q125K
11	ORF033: I37S, R88K, A117T
12	ORF039: C144F, A150S, D215E, Y222F
13	ORF112: <u>V22I</u> , 93Ndel, 94Ddel, N95D; ORF113: <u>A53T</u> , <u>F283S</u>

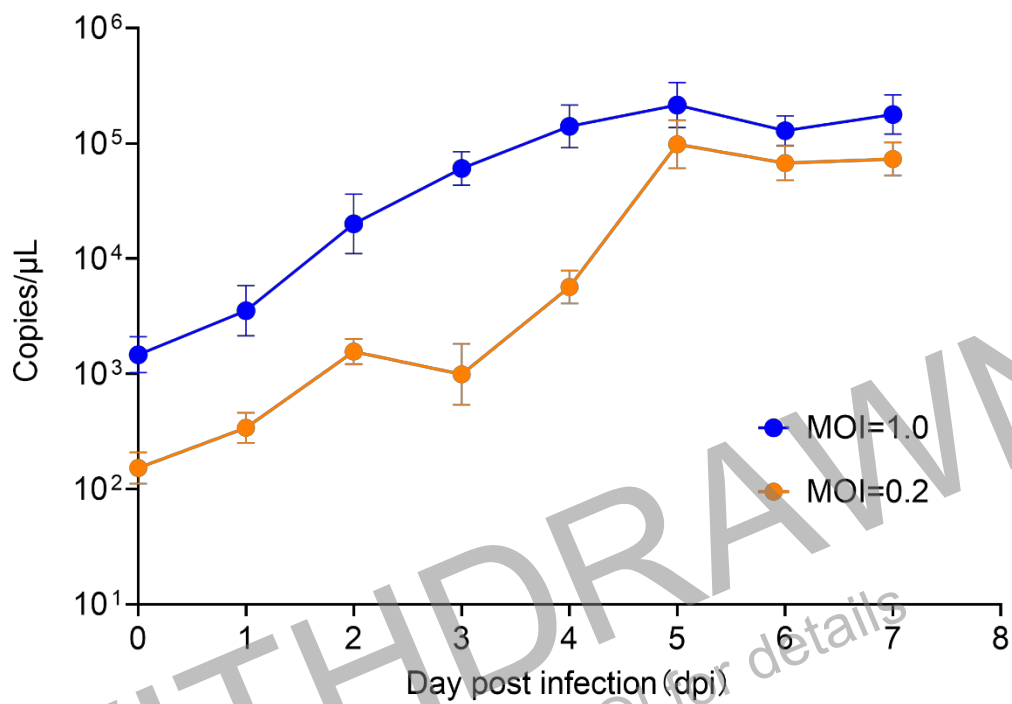
<sup>a</sup> Some minor recombination events in the genome of GD01/2020 could be not predicted; the amino acid changes also existing in the genome of Russia/Saratov/2017 (MH646674) are underlined; other over 16 proteins involved in these major predicted recombination events without amino acid sequence difference between the two parents are not listed in this table.



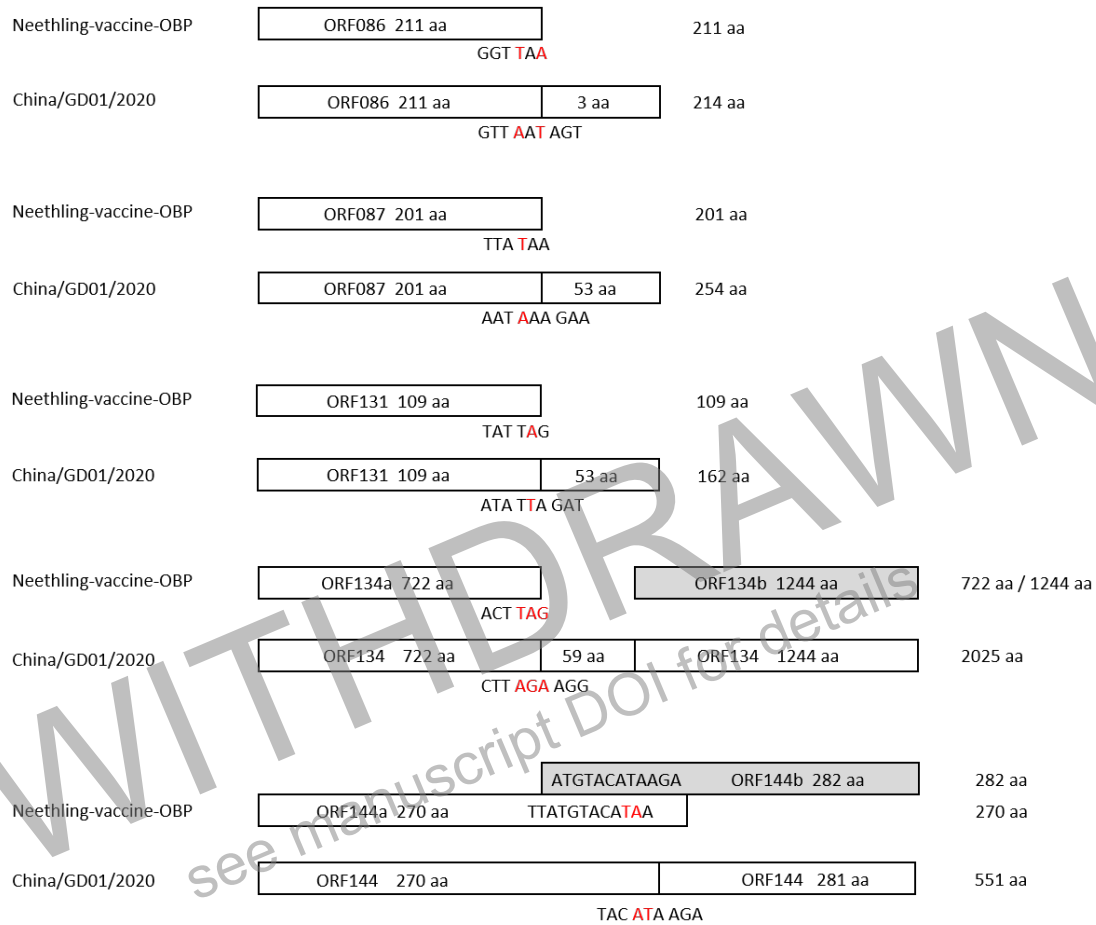
**Appendix Figure 1. Dates and affected provinces of the LSDV outbreaks in China in 2019 and 2020.** All data were from the Ministry of Agriculture and Rural Affairs of China ([http://www.xmsyj.moa.gov.cn/yqfb/202007/t20200715\\_6348686.htm](http://www.xmsyj.moa.gov.cn/yqfb/202007/t20200715_6348686.htm)).



**Appendix Figure 2. Detection of the GD01/2020 in clinical samples by the qPCR.** Numbers above each group represent the numbers of positive samples versus total samples.



**Appendix Figure 3. Growth kinetics of GD01/2020.** Each point is shown as the mean  $\pm$  SD of three independent experiments.



**Appendix Figure 4.** Termination codons of five genes of GD01/2020 changed as compared with the Neethling vaccine strain OBP.